Arch. Metall. Mater. **71** (2026), 1, 317-322

DOI: https://doi.org/10.24425/amm.2026.157795

NGUYEN THUY NGAN[1,3], PHAN QUOC PHU[2,3], LUONG THI QUYNH ANH[1,3*]

THE EFFECT OF POLYETHYLENE GLYCOL (PEG) CONCENTRATION OF SUPER-PARAMAGNETIC $Zn_{0.8}Ni_{0.2}Fe_2O_4$ FERRITES NANOPARTICLES ON MAGNETIC PROPERTIES (M_S, H_C)

In this study, super-paramagnetic $Zn_{0.8}Ni_{0.2}Fe_2O_4$ ferrite nanoparticles were synthesized simultaneously with the PEG layers covering using the hydrothermal method. The X-ray Diffraction (XRD) was used to determine the structure of ferrite, the Scanning Electron Microscope (SEM) indicated that the average size of particles was approximately 10.7-13.1 nm, respectively, and PEG affected to change the average size of the particle, besides, they can be a good candidate for the agglomeration of the particles, this lead to keep the super-paramagnetic state of them. Additionally, the Vibrating Samples Magnetometer (VSM) revealed that the magnetization saturation M_s of samples reached the highest value (28.47 emu/gr) with 0.15 g/5 ml PEG concentration. The high saturation magnetization of super-paramagnetic $Zn_{0.8}Ni_{0.2}Fe_2O_4$ ferrite nanoparticles promises a good ability for applications such as microwave absorbing materials, X-ray clothing protection, MRI contrast image enhancement, target drug delivery, and gas sensors.

Keywords: PEG concentration; ferrite nanoparticles; magnetic properties

1. Introduction

Magnetic materials have created great expectations in the last few years [1-3]. Magnetic materials demonstrate excellent ability in microwave absorbing materials when they reach a superparamagnetic state (the particles with an average size less than 10 nm, and the coercive force H_c, the remanence M_r towards zero value) [4-6]. Besides, the superparamagnetic materials exhibit their high potential applications such as drug target delivery, MRI contrast enhancement, gas sensors, cancer treatment, magnetic nanofluids, stealth painting layers in the military [7-13], and so on. To keep the superparamagnetic state of ferrites, surfactant plays an important role in preventing agglomeration, good stability, and uniform particle sizes. Applying in the biomedical field requires non-toxicity and compatibility with the human body. Polyethylene glycol (PEG) is the best candidate for coating these superparamagnetic particles [12,14,15].

In application for cancer treatment, V.J. Sawant and colleagues studied PEG coating of zinc ferrite and cobalt towards breast cancer treatment [12], $CoFe_2O_4$ and $ZnFe_2O_4$ nanoparticles were surface functionalized with PEG and Chitosan, the effects of PEG and Chitosan coating over ferrites for Curcumin release have been elaborated, and the Chitosan coated Curcumin loaded Zinc ferrite nanohybrid exhibited higher drug delivery and anticancer effects. Besides, the effect of the PEGylation process on the magnetic properties and biocompatibility of the synthesized nanoparticles was also studied by Sedigheh Cheraghali and colleagues [14]. The results show that the PEG-coated MnZn ferrite nanoparticles with hierarchical structure synthesized in the study can be considered as an MRI contrast agent at concentrations between 0.1 and 0.3 mg/ml.

There are various techniques adopted for the synthesis of nanosized zinc nickel ferrite, including co-precipitation [17], sol-gel techniques, and hydrothermal methods. In this study, we use the co-precipitation method combined with hydrothermal conditions to synthesize at a low temperature, to investigate the effects of PEG concentration on $Zn_{0.8}Ni_{0.2}Fe_2O_4$ nanoparticle's magnetic properties.

[1] HO CHI MINH CITY UNIVERSITY OF TECHNOLOGY (HCMUT), FACULTY OF MATERIALS TECHNOLOGY DEPARTMENT OF METALLURGY AND ALLOYS MATERIALS, 268 LY THUONG KIET STREET, DISTRICT 10, HO CHI MINH CITY, VIETNAM
[2] HO CHI MINH CITY UNIVERSITY OF TECHNOLOGY (HCMUT), DEPARTMENT OF POLYMERS MATERIALS, FACULTY OF MATERIALS TECHNOLOGY, 268 LY THUONG KIET STREET, DISTRICT 10, HO CHI MINH CITY, VIETNAM
[3] VIETNAM NATIONAL UNIVERSITY HO CHI MINH CITY, LINH TRUNG WARD, THU DUC CITY, HO CHI MINH CITY, VIETNAM
* Corresponding author: ltqanh@hcmut.edu.vn

© 2026. The Author(s). This is an open-access article distributed under the terms of the Creative Commons Attribution License (CC-BY 4.0). The Journal license is: https://creativecommons.org/licenses/by/4.0/deed.en. This license allows others to distribute, remix, modify, and build upon the author's work, even commercially, as long as the original work is attributed to the author.

2. Experimental procedure

2.1. Chemicals

All chemicals used were $FeCl_3.6H_2O$, $ZnCl_2$, $NiCl_2.6H_2O$, NH_4OH, and PEG purchased from Sigma Aldrich (USA). Only ethanol was obtained from Xylong (China).

2.2. The synthesis process of super-paramagnetic $Zn_{0.8}Ni_{0.2}Fe_2O_4$ ferrite nanoparticles

The pure Zinc, Nickel, and Ferric salts were dissolved in doubly distilled water to get a solution with a concentration of 0.1 M. Then, the PEG solution was dropped by drop to the above solution. The mixture was then heated to 60°C under stirring at 500 rpm. Next, the 25% ammonia solution was added to precipitate the mixtures. Add PEG solution before the ammonia solution to prevent agglomeration of particles when precipitation occurs. The hydroxides of Zinc, Nickel, and Ferric were formed. After that, they were poured into a Teflon stainless steel autoclave and heated to 140°C in 6 hours. Finally, the mixture was washed with ethanol to remove the impurities and dried at 100°C for 4 hours. The superparamagnetic $Zn_{0.8}Ni_{0.2}Fe_2O_4$ ferrite nanoparticles were collected, displaying a brown color. Fig. 1 illustrated all the steps of the process.

2.3. Characterizations

X-ray diffraction (XRD) method was used to analyze the structure of super-paramagnetic ferrites $Zn_{0.8}Ni_{0.2}Fe_2O_4$ nanoparticles (Bruker D8 diffractometer) with Cu-K_α radiation. Fourier Transform Infrared (FTIR) Spectroscopy (Model: TENSOR37-BRUKER) was used to confirm the chemical bonds present in the samples. The morphological analysis was carried out by Scanning Electron Microscope (SEM, S-4800). The magnetic properties of samples were determined using a Vibrating Sample Magnetometer (VSM, MICRO SENSE 3474-140).

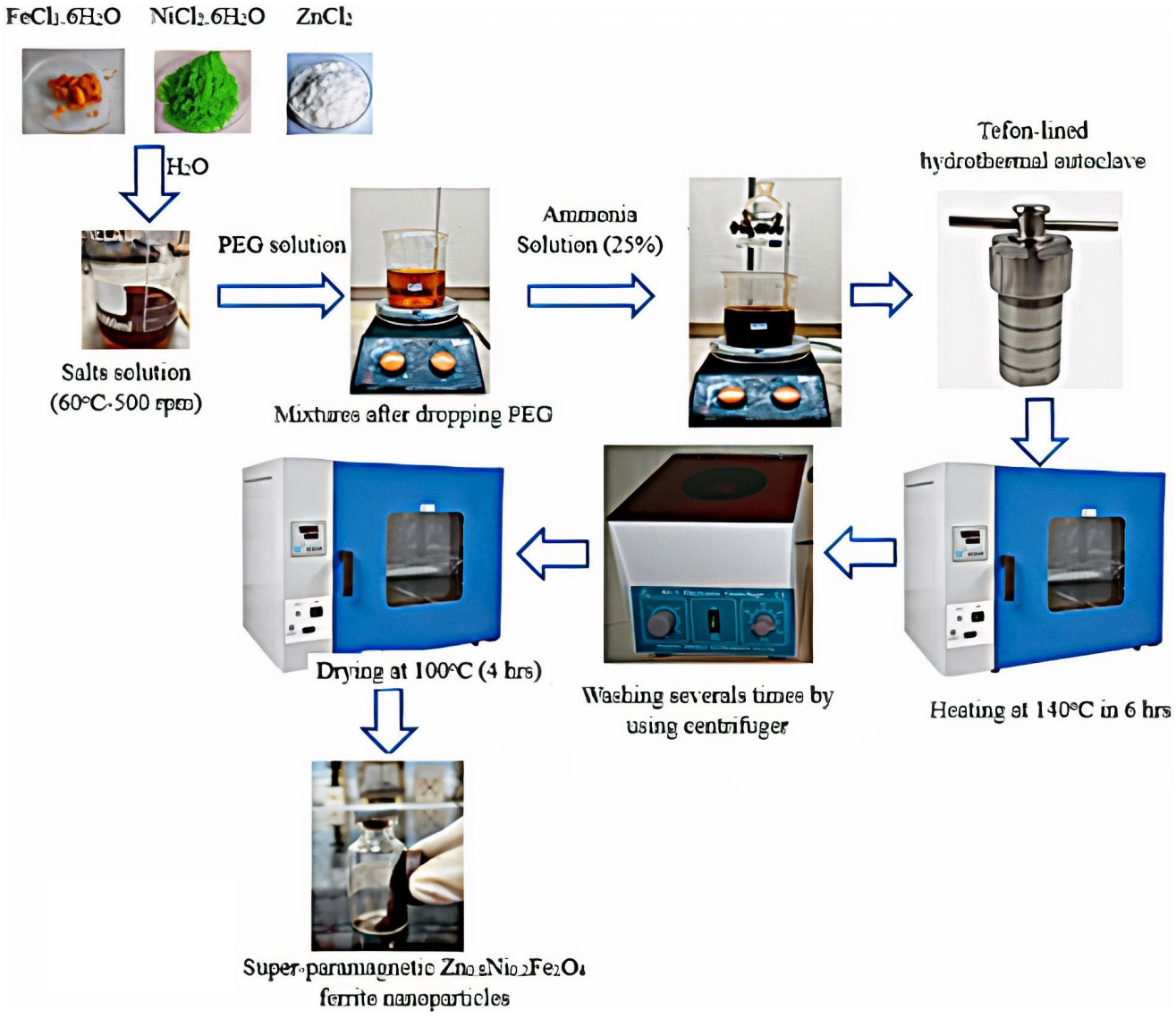

Fig. 1. The super-paramagnetic $Zn_{0.8}Ni_{0.2}Fe_2O_4$ ferrite nanoparticles process

3. Results and discussions

3.1. The effect of the PEG's concentration on the structure and nanoparticle size of super-paramagnetic $Zn_{0.8}Ni_{0.2}Fe_2O_4$ ferrite nanoparticles

Fig. 2 shows the X-ray diffraction spectrum of $Zn_{0.8}Ni_{0.2}Fe_2O_4$ nanoparticles with PEG's different concentrations from 0.075 g/5 ml to 0.2 g/5 ml. XRD spectrum is taken with a scanning angle from 20°- 70°, the spectrum clearly shows 6 peaks: (220), (311), (400), (422), (511), (440) of 5 samples. Based on the peak angles of the spectrum, we can conclude that the XRD spectrum has a pretty good crystallization degree, corresponding to the standard (JCPDS 52-0277) for the Zinc Nickel spinel X-ray diffraction pattern.

The crystallite size of each composition was then determined by the Scherrer relation [17]:

$$D = \frac{K.\lambda}{\beta.\cos\theta}$$

where K is constant, taken by 0.89; D is the crystallite size, λ is the X-ray wavelength, β is the full width at half maximum (FWHM) measured in radians, and θ is the Bragg angle. The values of XRD parameters are listed in TABLE 1.

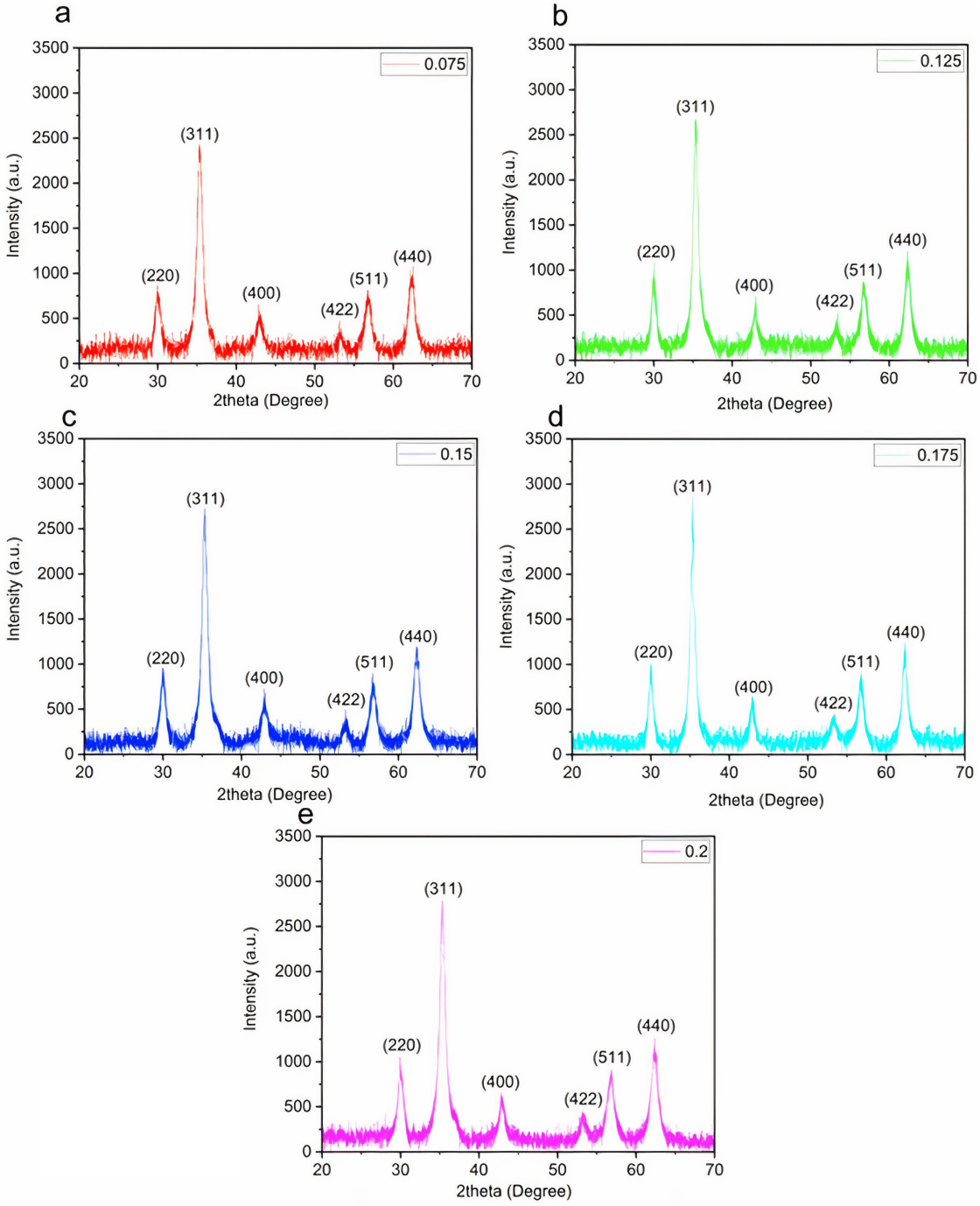

Fig. 2. XRD patterns of $Zn_{0.8}Ni_{0.2}Fe_2O_4$ nanoparticles ferrites synthesized with PEG's different concentrations: a. 0.075 g/5 ml; b. 0.125 g/5 ml; c. 0.15 g/5 ml; d. 0.175 g/5 ml; e. 0.2 g/5 ml

TABLE 1

The 2θ, FWHM, and average crystallite size of $Zn_{0.8}Ni_{0.2}Fe_2O_4$ nanoparticles

PEG's concentration samples (g/ml)	2θ (°)	β (FWHM) in radian	Average crystallite size (nm)
0.075g/5ml	17.68	0.0175	8.3
0.125g/5ml	17.68	0.0168	9.2
0.15g/5ml	17.67	0.0134	10.3
0.175g/5ml	17.67	0.0142	10.2
0.2g/5ml	17.68	0.0161	9.1

The average crystallite size rises from 8.3 nm to 10.3 nm when the PEG's concentration increases from 0.075 g/5 ml to 0.15 g/5 ml. Then, the crystalite size decreases from 10.3 nm to 9.1 nm. The values of the calculated crystallite size from Scherrer's formula varied from 9.1 nm to 10.3 nm with the change in PEG concentration. So, adding PEG's concentration reaches the highest average crystallite size at 0.15 g/5 ml.

The FTIR was used to confirm the bonding of samples with and without PEG. In Fig. 3 with PEG, the wave number displayed at 1000.92 cm^{-1} is a stretching vibration of the C-O group [18]. In addition, the wavenumber at 3405.9 cm^{-1} was related to the stretching vibration of the –OH group (hydroxyl)

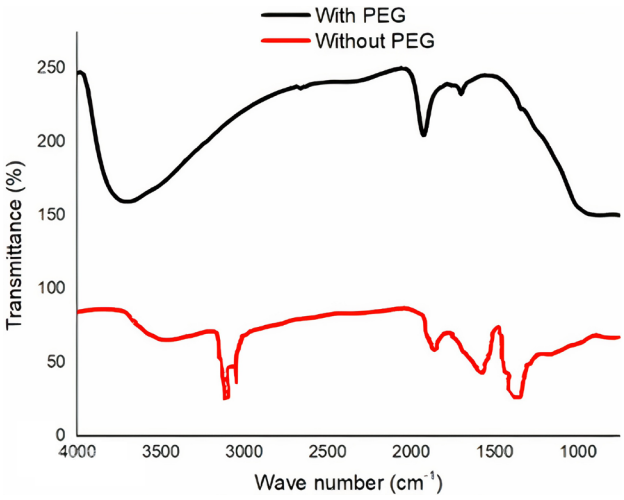

Fig. 3. FTIR of samples with and without PEG

[19,20], a common peak in PEG. So, the FTIR spectrum confirmed the PEG appearance.

Fig. 4 displays the size distribution of $Zn_{0.8}Ni_{0.2}Fe_2O_4$ nanoparticles after covering by PEG. And, the aim of using PEG layers is to prevent the agglomeration of ferrite nanoparticles and keep

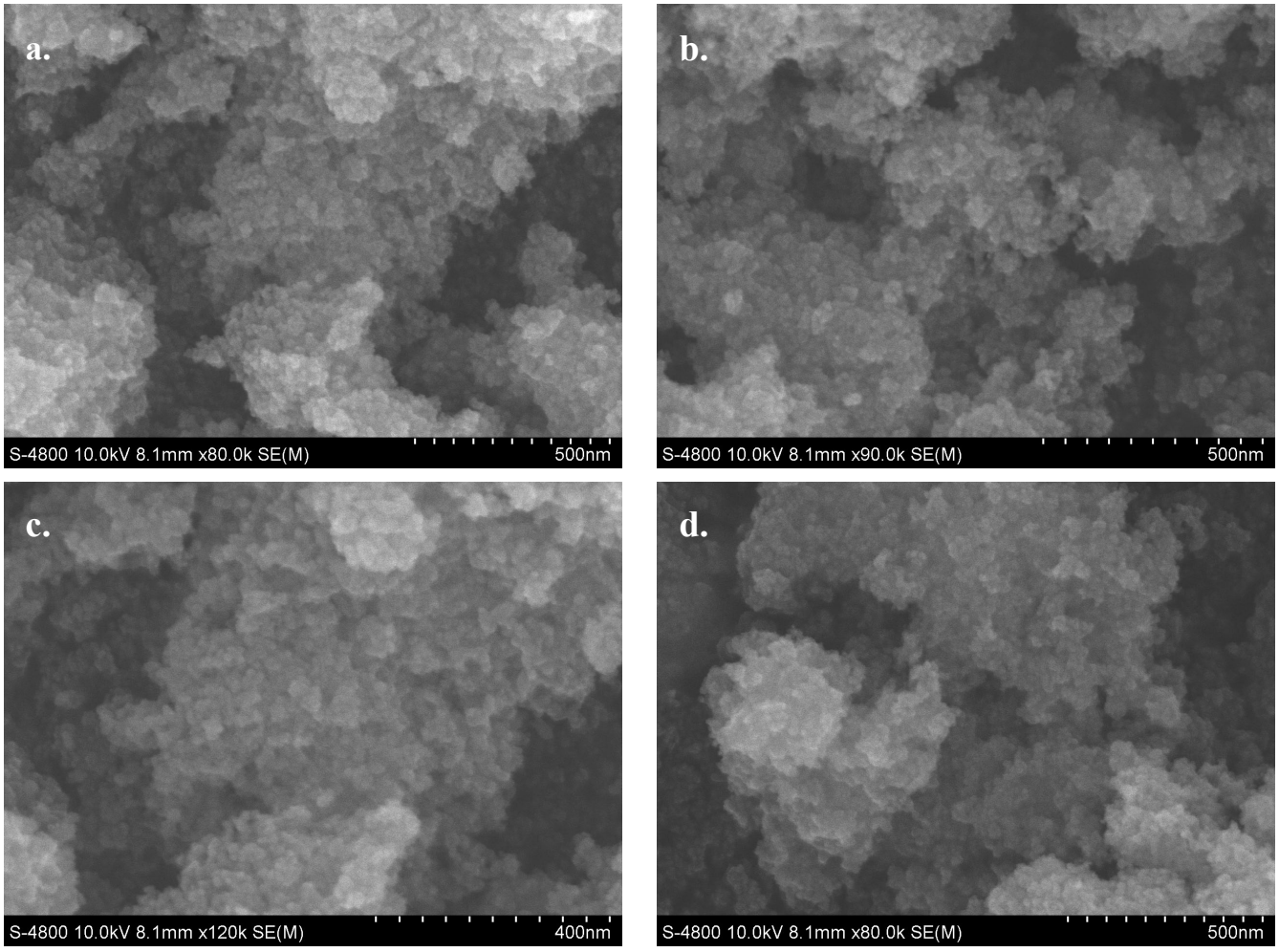

Fig. 4. SEM images of super-paramagnetic $Zn_{0.8}Ni_{0.2}Fe_2O_4$ ferrites nanoparticles with PEG concentration of a. 0.075 g/5 ml; b.0.125 g/5 ml, c. 0.15 g/5 ml, d. 0.175 g/5 ml and e. 0.2 g/5 ml

them stable in a super-paramagnetic state [14]. The SEM analyses show the spherical morphology of $Zn_{0.8}Ni_{0.2}Fe_2O_4$ nanoparticles, and the average size is approximately 10.7-13.1 nm, the addition of PEG's concentration (from 0.075 g/5 ml to 0.15 g/5 ml) lead to the increase of the size of $Zn_{0.8}Ni_{0.2}Fe_2O_4$ nanoparticles, respectively [21]. The average nanoparticle size of samples with 0.175 g/5 ml and 0.2 g/5 ml were 12.4 and 12.1 nm, with a variation of 0.1 nm. In conclusion, the increase in the PEG concentration does not highly affect the average nanoparticle size. In addition, the small average size leads to the one direction of the particle, respectively.

3.2. The effect of PEG's concentration on magnetic properties of super-paramagnetic $Zn_{0.8}Ni_{0.2}Fe_2O_4$ ferrite nanoparticles

The magnetic properties of super-paramagnetic $Zn_{0.8}Ni_{0.2}Fe_2O_4$ ferrite nanoparticles are displayed in Fig. 5 and TABLE 2. It is noted that the M_s value of super-paramagnetic $Zn_{0.8}Ni_{0.2}Fe_2O_4$ ferrite nanoparticles increased (19.69 to 28.47 emu/gram) with increasing PEG's concentration from 0.075 g/5 ml to 0.15 g/5 ml, and then, decrease to 26.95 emu/gr with increasing PEG's concentration to 0.2 g/5 ml. Compared to the covering layers of oleic acid and 1-pentanol as we had studied before [16,22], the PEG layers demonstrated the highest M_s value with the same heating temperature (140°C).

TABLE 2 indicates that the PEG layers are not affected by the super-paramagnetic state of $Zn_{0.8}Ni_{0.2}Fe_2O_4$ ferrite nanoparticles. All samples exhibit a coercivity force (H_c) and remanent magnetization (M_r) that reach zero, indicating they have achieved a super-paramagnetic state. The maximum magnetization saturation was at 0.15 g/5 ml PEG's concentration. In our previous study [23], the super-paramagnetic state of $Zn_{0.8}Ni_{0.2}Fe_2O_4$ ferrite nanoparticles had been applied to microwave-absorbing materials. It reached a very high microwave absorption percentage, which is also indicated in another study [24].

TABLE 2

Magnetic properties of super-paramagnetic $Zn_{0.8}Ni_{0.2}Fe_2O_4$ ferrites nanoparticles with different PEG concentrations

PEG's concentration samples (g/ml)	Coercivity force H_c (Oe)	Saturation Magnetization M_s (emu/gr)	Remanent Magnetization M_r (emu/gr)
0.075 g/5 ml	0.018	19.69	6.9×10^{-6}
0.125 g/5 ml	0.009	27.83	9.1×10^{-6}
0.15 g/5 ml	0.009	28.47	3.3×10^{-6}
0.175 g/5 ml	0.025	28.15	11×10^{-6}
0.2 g/5 ml	0.023	26.95	7.7×10^{-6}

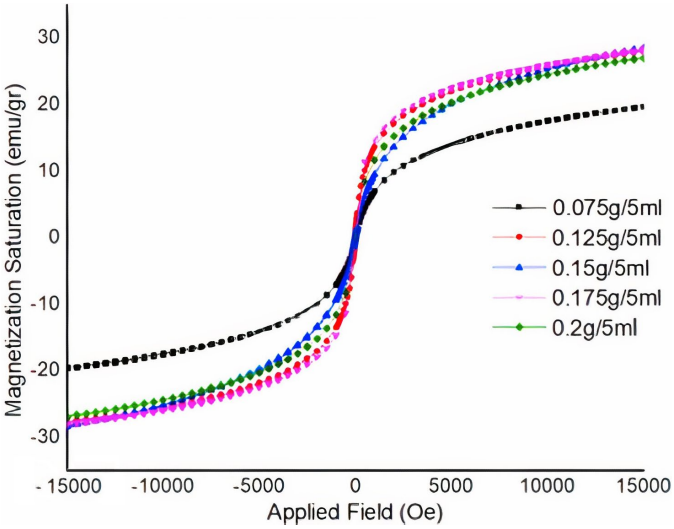

Fig. 5. Magnetization curves of super-paramagnetic $Zn_{0.8}Ni_{0.2}Fe_2O_4$ ferrite nanoparticles with different PEG concentrations

4. Conclusions

PEG layers cover the super-paramagnetic $Zn_{0.8}Ni_{0.2}Fe_2O_4$ ferrite nanoparticles. The study demonstrated that the magnetization saturation value increased with increasing PEG's concentration from 0.075 g/5 ml to 0.15 g/5 ml, the highest magnetization saturation value reached 28.47 emu/gr with 0.15 g/5 ml PEG's concentration. The high value of magnetization saturation promises a good ability for microwave-absorbing materials, MRI contrasts image enhancement, target drug delivery, and X-ray clothing protection.

Acknowledgments

We acknowledge Ho Chi Minh City University of Technology (HCMUT), VNU-HCM, for supporting this study.

REFERENCES

[1] M.A. Dar, J. Shah, W.A. Siddiqui, R.K. Kotnala, Appl. Nanosci. **4**, 675 (2014). DOI: https://doi.org/10.1007/s13204-013-0241-x

[2] C. Caizer, M. Stefanescu, J. Phys. D: Appl. Phys. **35**, 3035 (2002). DOI: https://doi.org/10.1088/0022-3727/35/23/301

[3] M. Darko, D. Miha, J. Am. Ceram. Soc. **82**, 1113 (1999). DOI: https://doi.org/10.1631/jzus.2005.b0580

[4] L. Kong, X. Yin, X. Yuan, Y. Zhang, X. Liu, L. Cheng, L. Zhang, Carbon. **73**, 185 (2014). DOI: https://doi.org/10.1016/j.carbon.2014.02.054

[5] Z. Jun, T. Peng, W. Sen, X. Jincheng, Appl. Surf. Sci. **255**, 4916 (2009). DOI: https://doi.org/10.1016/j.apsusc.2008.12.036

[6] J.B. Kim, S.K. Lee, C.G. Kim, Composi. Sci. and Tech. **68**, 2909 (2008). DOI: https://doi.org/10.1016/j.compscitech.2007.10.035

[7] A.H. Habib, C.L. Ondeck, P. Chaudhary, M.R. Bockstaller, M.E. McHenry, J. Appl. Phys. **103**, 07A307 (2008). DOI: https://doi.org/10.1063/1.2830975

[8] R.B. Kamble, V.L. Mathe, Sensors and Actuators. **131**, 205 (2008). DOI: https://doi.org/10.1016/j.snb.2007.11.003

[9] H. Basti, L.B. Tahar, L.S. Smiri, F. Herbst, M.J. Vaulay, F. Chau, S. Ammar, S. Benderbous, J. of Col. and Inter. Sci. **341**, 248 (2010). DOI: https://doi.org/10.1016/j.jcis.2009.09.043

[10] V.Y. Mehmet, M. Anna, M. Zdravka, Pharm. Res. **29**, 1180 (2012). DOI: https://doi.org/10.1007/s11095-012-0679-7

[11] N.G. Imam, M. AbouHasswa, G. Aquilanti, S.I.E. Dek, N. Okasha, A.A.G.A. Shahawy, J. Mater. Res. and Tech. **15**, 4130 (2021). DOI: https://doi.org/10.1016/j.jmrt.2021.09.143

[12] V.J. Sawant, S.R. Bamane, R.V. Shejwal, S.B. Patil, J of Mag. and Mag. Mater. **417**, 222 (2016). DOI: https://doi.org/10.1021/acs.chemmater.2c01568

[13] K. Ajith, I.V.M. Enoch, A.B. Solomon, A.S. Pillai, Mater. Today: Proceedings. **27**, 107 (2020). DOI: https://doi.org/10.1016/j.matpr.2019.09.014

[14] S. Cheraghali, G. Dini, I. Caligiuri, M. Back, F. Rizzolio, Nanomaterials. **13**, 452 (2023). DOI: https://doi.org/10.3390/nano13030452

[15] S. Akhtar, Q. Khan, S. Anwar, G. Ali, M. Maqbool, M. Khan, S. Karim and L.A. Gao, Nanos. Res. Let. **14**, 386 (2019).

[16] A.T.Q. Luong, D.V. Nguyen, Inter. J. of Mater. Res. **6**, 555 (2018). DOI: https://doi.org/10.3139/146.111629

[17] B.D. Cullity, "Elements of X-ray Diffraction" Pearson New International Edition, London, 1959.

[18] M. Sari, Y. Yusuf, IOP Conf. Ser. Mater. Sci. Eng. **432**, 012046 (2018). DOI: https://doi.org/10.1088/1757-899x/432/1/012046

[19] H. Hao, Y. Wang, B. Shi, Water. Res. **155**, 1 (2019). DOI: https://doi.org/10.1016/j.watres.2019.01.049

[20] D.B. Nugroho, A. Rianjanu, K. Triyana, A. Kusumaatmaja, R. Roto, Results Phys. **15**, 102680 (2019). DOI: https://doi.org/10.1016/j.rinp.2019.102680

[21] N.G. Imam, M. A. Hasswa, A. Giuliana, S.I. El. Dek, N. Okasha, A.G. Ahmed, A. Shahawy, J. of Mater. Res. and Tech. **15**, 4130 (2021).

[22] A. Nuruddin, F.F. Diba, A.G. Saputro, B. Yuliarto, A. Ramelan, Mater. Res. Exp. **8**, 036102 (2021). DOI: https://doi.org/10.1016/j.jallcom.2015.05.146

[23] T.Q.L. Anh, V.N. Dan, Appl. Phys. A: Mater. Sci and Proc. **126**, 67 (2020). DOI: https://doi.org/10.1007/s00339-019-3251-z

[24] X. Wu, W. Wang, F. Li, S. Khaimanov, N. Tsidaeva, M. Lahoubi, Appl. Surf. Sci. **389**, 1003 (2016). DOI: https://doi.org/10.1016/j.apsusc.2016.08.053